CHEMISTRY
A EUROPEAN JOURNAL

ChemPubSoc
Europe

DOI: 10.1002/chem.201202890

Mechanism of Ketone Allylation with Allylboronates as Catalyzed by Zinc Compounds: A DFT Study

Weiyi Li, Zhishan Su, and Changwei Hu*[a]

Abstract: The mechanism of the allylation reaction between 4-chloroacetophenone and pinacol allylboronates catalyzed by $ZnEt_2$ with alcohols was investigated using density functional theory (DFT) at the M05-2X/6-311++G(d,p) level. The calculations reveal that the reaction prefers to proceed through a double γ-addition stepwise reaction mechanism rather than a Lewis acid-catalyzed concerted one. The intermediate with a four-coordinated boron center, which is formed through proton transfer from EtOH to the ethyl group of $ZnEt_2$ mediated by the boron center, is the active species and an entrance for the catalytic cycle. The latter is composed of three elementary steps: 1) boron to zinc transmetalation leading to the formation of allylzincate species, 2) electrophilic addition of ketone to allylzincate species, and 3) generation of the final product with recovery of the catalyst. The boron to zinc transmetalation step has the largest energy barrier of 61.0 kJ mol^{-1} and is predicted to be the rate-determining step. The calculations indicate that the additive EtOH plays important roles both in lowering the activation free energy for the formation of the four-coordinated boron active intermediate and in transforming the low catalytic activity $ZnEt_2$ into high activity zinc alkoxide species. The alcohols with a less sterically encumbering R group might be the effective additives. The substituted groups on the allylboronates might primarily affect the boron to zinc transmetalation, and the allylboronates with substituents on the C_γ atom is poor in reactivity. The comparison of the catalytic effect between the zinc compounds investigated suggest that $Zn(OEt)_2$, $Zn(OH)_2$, and ZnF_2 exhibit higher catalytic efficiency for the boron to zinc transmetalation due to the activation of the B–C_α bond through orbital interactions between the p orbitals of the EtO, OH, F groups and the empty p orbital of the boron center.

Keywords: additives · allylation · density functional calculations · reaction mechanisms · zinc

Introduction

Allylation reactions are a very convenient and efficient method to construct homoallylic alcohols, which are valuable building blocks and versatile intermediates in the organic syntheses of many biologically active molecules such as macrolides, polyhydroxylated nature products, and polyether antibiotics.[1] In the last two decades, considerable efforts have been invested in developing effective allylating reagents and catalysts to obtain homoallylic alcohols in terms of high yield and selectivity. Experimentally, allylhalides,[2] allylsilanes,[3] allylstannanes,[4] and allylboronates[5] have been reported to be effective allylating reagents for the allylation of carbonyl compounds. Among these allylating reagents, allylboronates with high reactivity and non-toxicity have been established as one of the most widely used allylating reagents.

For the allylation reaction between allylboronates and carbonyl compounds, Lewis acids, Brønsted acids, and metal complexes have been successfully employed as efficient catalysts. In early years, the research groups of Hall and Miyaura reported Lewis acids-catalyzed allylation of aldehydes with allylboronates.[6] The reaction rate was greatly accelerated in the presence of $Sc(OTf)_3$, $Cu(OTf)_2$, and $AlCl_3$. Sakata and Fujimoto carried out theoretical calculations on the $AlCl_3$-catalyzed allylation reaction between pinacol allylboronates and benzaldehyde at the B3LYP/6-311G-(d,p) level.[7] The results of the calculation indicated that the reaction went through a concerted mechanism via a six-membered ring transition state with lower activation energy in the presence of $AlCl_3$. The calculations also demonstrated the electrophilic boronates activation mechanism proposed by Hall and co-workers in which $AlCl_3$ is coordinated to one of two oxygen atoms in the boronate.[6c] Meanwhile, the interaction frontier orbitals (IFOs) analysis suggested that $AlCl_3$ attached to the oxygen atom of allylboronates strengthened the electrophilicity of the boron center and weakened the nucleophilicity of the C=C bond.

In 2005, Rauniyar and Hall discovered the achiral protic acid as Brønsted acids to catalyze the allylation of aldehydes with 2-alkoxycarbonyl allylboronates,[8a] and then they found that the combination of C_2-symmetric chiral diols with $SnCl_4$ as Brønsted acids resulted in high catalytic activity and

[a] Dr. W. Li, Z. Su, Prof. Dr. C. Hu
Key Laboratory of Green Chemistry & Technology
Ministry of Education, College of Chemistry
Sichuan University (P. R. China)
Fax: (+86) 28-8541-1105
E-mail: gchem@scu.edu.cn
chwehu@mail.sc.cninfo.net

Supporting information for this article is available on the WWW under http://dx.doi.org/10.1002/chem.201202890.

enantioselectivity.[8b,c] Jain and Antilla reported the use of a chiral BINOL-derived phosphoric acid as Brønsted acids catalyst for the allylboration of aldehydes with the allylboronic acid pinacol ester, which gave the products with good yields and enantioselectivity.[9] Goodman and co-workers studied the mechanism of such reaction by means of DFT and ONIOM calculations.[10] Their calculations indicated that the reaction preceded also through a concerted mechanism, in which C–C bond formation and B–C bond cleavage occurred simultaneously. The hydrogen-bonding interaction between the catalyst hydroxyl group and the pseudoaxial oxygen of the cyclic boronates as well as the stabilizing interaction from the phosphoryl oxygen of the catalyst to the formyl hydrogen of the aldehydes help to lower the energy of the transition state and provide extra rigidity to the system.

In addition, as one kind of useful and powerful catalysts, metal complexes have also attracted much attention in this field. A number of metals, such as In,[11] Cu^{I},[12] Ni^{II},[13] and Zn^{II}[14] have been used in this reaction. Among these metal-complex catalysts, zinc compounds are widely applied owing to their high catalytic activities and low costs. Kobayashi and co-workers reported ZnF_2 and $Zn(OH)_2$-catalyzed allylation of imines and aldehydes with pinacol allylboronates at room temperature.[14a,b] High regioselectivities in the formation of α-addition products were achieved using a combination of $Zn(OH)_2$ and a diamine ligand in aqueous media. An extended investigation indicated that the allylation of benzaldehyde with allyboronic acid 2,2-dimethyl-1,3-propanediol ester catalyzed by chiral bipyridine ligated with $Zn(OH)_2$ gave the corresponding products with excellent *syn* selectivity and good enantioselectivity.[14c] Based on the experimental observations, a double γ-addition mechanism was proposed, which was different from the Lewis acid and Brønsted acid-catalyzed concerted mechanism (in Scheme 1). The catalytic cycle involves the following steps: 1) formation of allylzincate active species through transmetalation from boron to zinc, 2) electrophilic addition of carbonyl compounds to allylzincate active species, and 3) hydrolysis of product intermediate with regeneration of the catalyst. Fandrick et al. studied the allylation reaction between ketones and a series of pinacol allylboronates catalyzed by $ZnCl_2$, $ZnBr_2$, and $ZnEt_2$.[14d] The experimental results showed that the reaction rate was significantly affected by the zinc compounds, the additives, the substituents on the allylboronates, and the solvents. It is interesting to note that the catalytic system composed of $ZnEt_2$ and additive EtOH was very efficient in accelerating the reaction rate and improving the yield of the product (Scheme 2).

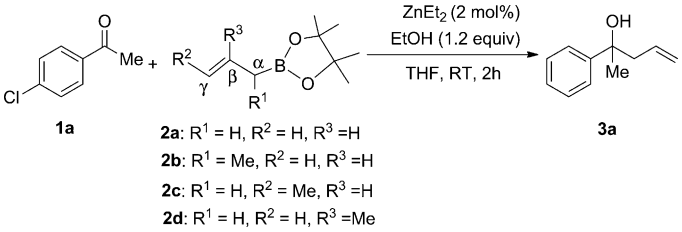

Scheme 2. $ZnEt_2$/EtOH-catalyzed allylation of 4-chloroacetophenone with pinacol allylboronates.

To the best of our knowledge, although the mechanisms of Lewis acid and Brønsted acid-catalyzed allylation reaction between allylboronates and aldehydes have been investigated theoretically, the computational studies on the mechanism of metal complexes-catalyzed allylation reaction are very limited so far. Zinc complexes-catalyzed allylation of carbonyl compounds with allylboronates represents one kind of metal-mediated allylation reaction and the catalytic mechanism has not yet been completely elucidated. The reaction between 4-chloroacetophenone (**1a**) and pinacol allylboronates (**2a**–**2d**) reported by Fandrick and co-workers (Scheme 2) provided a good reaction model for the quantum chemical study of zinc compounds-catalyzed mechanism of allylation of carbonyl compounds at molecular level. In the present work, DFT calculations were performed to investigate the reaction mechanism, the role of the EtOH additive, and the factors influencing the reaction rate. Furthermore, the catalytic effect of several simple zinc compounds including $Zn(OEt)_2$, $Zn(OH)_2$, ZnF_2, $ZnCl_2$, and $ZnBr_2$ for the present reaction system was also compared based on the theoretical calculations.

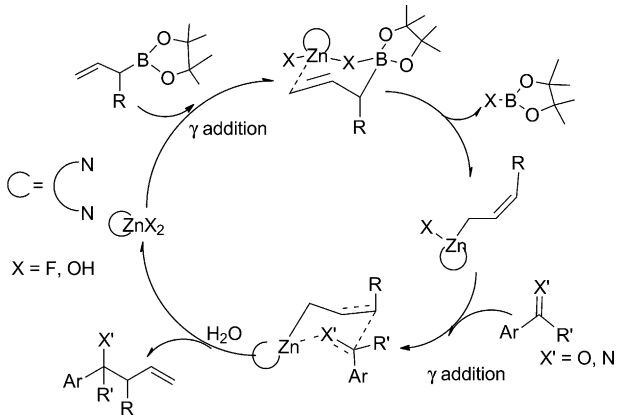

Scheme 1. Kobayashi's double γ-addition mechanism.

Computational Methods

Recently, the hybrid meta exchange-correlation function M05-2X developed by Zhao and Truhlar was demonstrated to outperform the popular B3LYP function in main group thermochemistry, kinetics, and noncovalent interactions within "medium-range" ($\leq$5 Å),[15] and was recommended as the most suitable method for the accurate geometry optimization and energetic calculations of zinc compounds.[16] Accordingly, the geometry optimization of all intermediates and transition states in the present system were performed using the M05-2X function with the 6-31G(d,p) basis set.[17] The vibrational frequencies were calculated at the same level to identify a minimum (no imaginary frequency) or first-order saddle-point (unique imaginary frequency) and perform zero-point vibrational energy (ZPVE) corrections. To obtain further insight into the electronic property of the present system, natural bond orbital (NBO)[18] analysis

was also performed on the optimized structures. Considering the effect of the solvent, the single-point energies in THF ($\varepsilon = 7.58$) at 298 K (experiment temperature) were calculated at the M05-2X/6-311++G(d,p) level by employing polarizable continuum model (PCM[19]). Unless otherwise specified, the Gibbs free energies at 298 K obtained by the combination of these single-point energies with Gibbs free energy corrections at the M05-2X/6-31G(d,p) level in the gas phase were used in the discussion. All calculations were performed using the Gaussian 03 programs.[20]

Results and Discussion

Initially, the uncatalyzed reaction between **1a** and **2a** was investigated. As shown in Figure 1, in the absence of catalyst, the reaction takes place via a concerted mechanism with a six-membered-ring transition state (*b*-**TS1**), in which the boron center of **2a** acts as a Lewis acid to activate ketone **1a**. In *b*-**TS1**, the phenyl group is located in equatorial position and the methyl group is in axial position. *b*-**TS1** bearing this equatorial chair conformation is energetically more favorable than those of the axial chair and boat conformation.[10] The Gibbs free energy of activation relative to the reactants (**1a**+**2a**) is calculated to be 106.1 kJ mol^{-1} at the M05-2X/6-311++G(d,p) level, which is similar to the theoretical results (125.8 kJ mol^{-1}) of the uncatalyzed allylation of benzaldehyde with **2a** by Sakata and Fujimoto at the B3LYP/6-311G(d,p) level.[7] This theoretical result is in agreement with the low reaction rate of the uncatalyzed allylboration observed in the experiment.[14d]

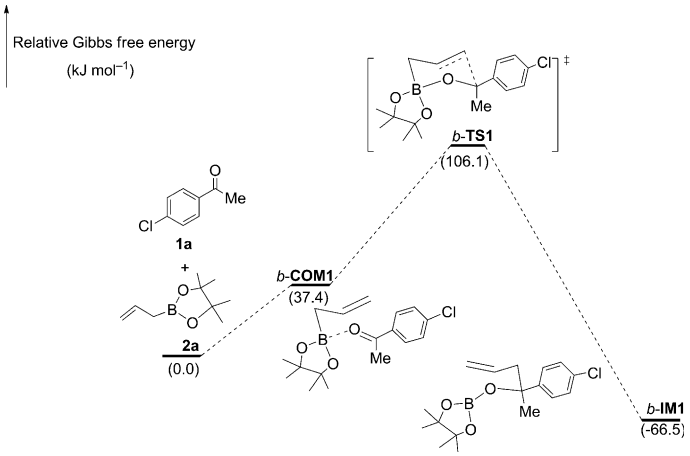

Figure 1. Energy profile of the uncatalyzed allylation of **1a** with **2a**. The relative Gibbs free energies in THF at the M05-2X/6-311++G(d,p) level are given in kJ mol^{-1}.

$ZnEt_2$-catalyzed reaction: In Fandrick's experiment, it was found that the additive EtOH played an important role in accelerating the reaction rate.[14d] To get a better understanding of the role of additive EtOH and to compare the reaction mechanisms with and without EtOH, the mechanism of the allylation between **1a** and **2a** catalyzed by $ZnEt_2$ alone was explored. For the $ZnEt_2$-catalzyed reaction, two possible reaction mechanisms (concerted and stepwise) were calculated (see Figure S1 in the Supporting Information). The energy profile of the two reaction pathways is presented in Figure 2.

The concerted pathway starts from the coordination of one oxygen atom in **2a** to $ZnEt_2$ with the formation of the

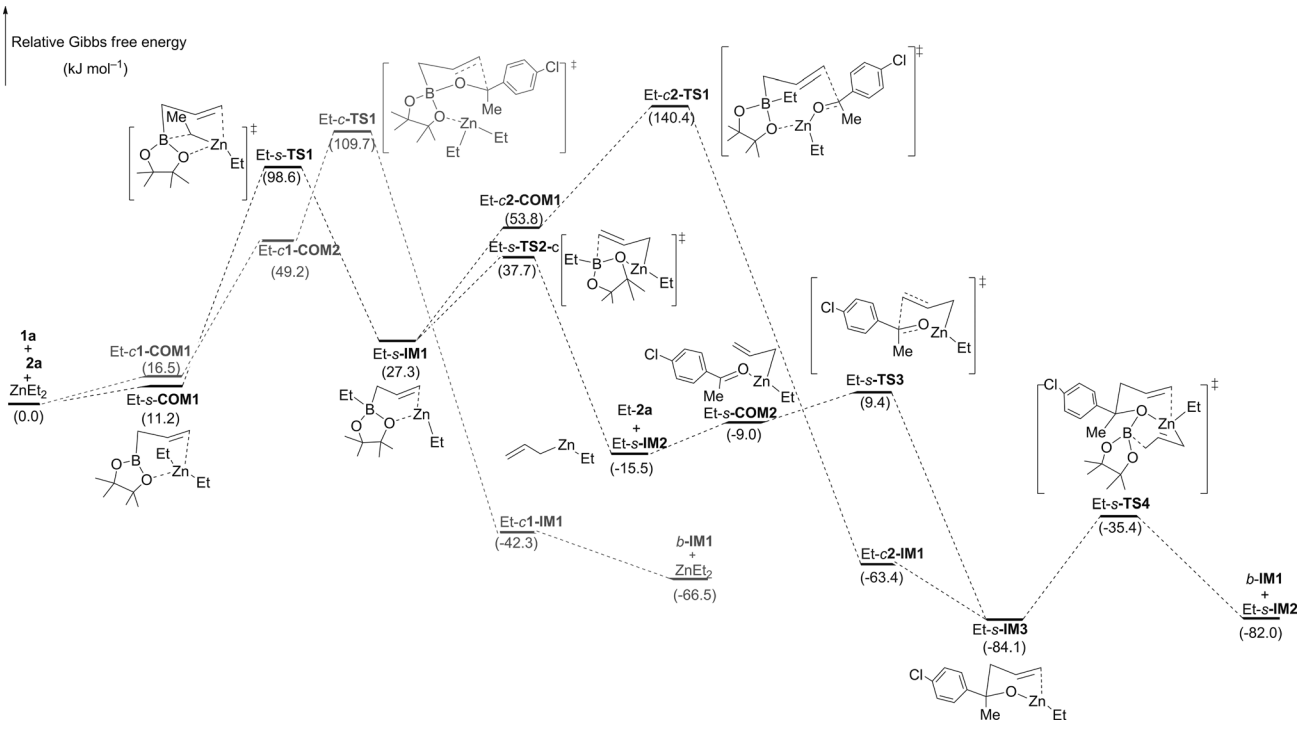

Figure 2. Energy profiles of $ZnEt_2$-catalyzed allylation of **1a** with **2a**. The relative Gibbs free energies in THF at the M05-2X/6-311++G(d,p) level are given in kJ mol^{-1}.

complex Et-*c*1-**COM1**. Next, **1a** approaches to the complexes Et-*c*-**COM1** to yield the ternary complex Et-*c*1-**COM2**. In Et-*c*1-**COM2**, NBO analysis shows that the Wiberg bond index of the B–C_α bond and the occupancy of antibonding orbital of BD*(σ)B–C_α are 0.857 and 0.021, respectively, which are comparable with those in free **2a** (0.878 and 0.019). Since the activation of the B–C_α bond by $ZnEt_2$ is poor, the electrophile attack of **1a** to allyl moiety via the concerted six-mebermed ring transition state Et-*c*1-**TS1** requires a higher Gibbs free energy of activation of 109.7 kJ mol^{-1}, which is 32.2 kJ mol^{-1} higher than that in $AlCl_3$-catalzyed allylation of benzaldehyde,[7] and comparable to that of the uncatalyzed reacion. This result suggests that $ZnEt_2$ exhibits poorer Lewis acid characteristics in catalyzing the allylation of ketones with allylboronates.

On the other hand, the reaction might alternatively take place along a stepwise pathway, which involves: 1) the boron to zinc transmetalation to generate allylzincate species, 2) the addition of **1a** to allylzincate species to yield the allylation product, and 3) the second boron to zinc transmetalation between the product intermediate and **2a** with the recovery of allylzincate species. As shown in Figure 2, the transmetalation step concerns the initial transfer of one ethyl group from $ZnEt_2$ to the boron center of **2a** with the formation of intermediate Et-*s*-**IM1** followed by the cleavage of the B–C_α bond with the insertion of zinc to the C_γ=C_β bond. Starting from the reactant complex Et-*s*-**COM1**, the transfer of ethyl group to boron center occurs via the four-mebermed ring transition state Et-*s*-**TS1**, which needs to surmount an energy barrier of 87.4 kJ mol^{-1} in Gibbs free energy. A similar transfer process has been reported in the theoretical calculations of the transmetalation between demethly(phenyl)boroxine and EtZnMe by Jimeno et al.[21] In the resulting intermediate Et-*s*-**IM1**, the four-coordinated boron center is formed, which decreases the charge on the boron atom from 1.190 *e* (in free **2a**) to 1.067 *e* and increases the charge on the zinc atom from 1.175 *e* (in free $ZnEt_2$) to 1.278 *e*. NBO analysis shows the remarkably decreased Wiberg bond index of the B–C_α bond (0.714 vs. 0.878 in free **2a**) and the increased occupancy of antibonding orbital of the BD*(σ) B–C_α bond (0.570 vs. 0.019), implying that the B–C_α bond is weakened and activated. From Et-*s*-**IM1**, the cleavage of the B–C_α bond with the insertion of zinc to C_γ=C_β bond can easily occur via Et-*s*-**TS2**. Both the chair and boat conformation transition states were located and marked as Et-*s*-**TS2**-c and Et-*s*-**TS2**-b, respectively. The chair conformation Et-*s*-**TS2**-c is 6.5 kJ mol^{-1} lower than the boat conformation transition states Et-*s*-**TS2**-c, and the energy barrier for overcoming Et-*s*-**TS2**-c is much lower (ΔG = 10.4 kJ mol^{-1}). Downhill from Et-*s*-**TS2**-c, allylzincate species Et-*s*-**IM2** is formed with the release of one ethylboronate. The charge on zinc atom increases further to 1.277 *e* and the global nucleophilicity N[22,23] increases from 2.33 to 3.75 eV. Then, the electrophile **1a** coordinates to the zinc center of Et-*s*-**IM2** with the formation of omplex Et-*s*-**COM2**. In Et-*s*-**COM2**, the activation of the C=O bond of **1a** can be verified by the increased population of the antibonding orbital BD*(π) C–O (0.188 vs. 0.115 in free **2a**) and the global electrophilicity ω[22,23] (3.31 eV vs. 3.11 eV in free **1a**). As a result, the electrophilic addition of **1a** to the allyl moiety can feasibly take place via the six-membered ring transition state Et-*s*-**TS3** with the lower energy barrier of 18.4 kJ mol^{-1}. As there is no existence of a proton donor in the reaction system, the external **2a** might participate in the boron to zinc transmetalation with Et-*s*-**IM3** via the transition state Et-*s*-**TS4**, which leads to the generation of allylzincate active species Et-*s*-**IM2** and the completion of the catalytic cycle.

Furthermore, it is found that the product intermediate Et-*s*-**IM3** might be also achieved from Et-*s*-**IM1** through the concerted transition state Et-*c*2-**TS1**. According to the NBO analysis, the B–C_α bond and the C=O bond of **1a** in Et-*c*2-**COM1** seem to be activated, however, the energy barrier for the addition of **1a** to allyl moiety via Et-*c*2-**TS1** is as high as 86.6 kJ mol^{-1}. This might be due to the fact that the eight-membered ring Et-*c*2-**TS1** suffers larger ring strain than six-membered ring transition states Et-*c*1-**TS1** and Et-*s*-**TS3**. The Gibbs free energy of Et-*c*2-**TS1** relative to the reactants (**1a**+**2a**+$ZnEt_2$) is 140.4 kJ mol^{-1}, which implies that the formation of product intermediate Et-*s*-**IM3** via the concerted transition state Et-*c*2-**TS1** is unfavorable with respect to thermodynamics and kinetics.

In summary, as compared to the concerted pathway, the active Gibbs free energy of the stepwise pathway is lowered by 11.1 kJ mol^{-1}, indicating that the allylation of **1a** with **2a** catalyzed by $ZnEt_2$ prefers to undergo the stepwise pathway, which is similar to the double γ-addition mechanism proposed by Kobayashi and co-workers in the $Zn(OH)_2$ and ZnF_2-catalyzed allylation of aldehydes and imines.[14a–c] For the stepwise pathway, the transfer of one ethyl group from $ZnEt_2$ to the boron center of **2a** possesses the largest energy barrier (87.4 kJ mol^{-1}) and the Et-*s*-**TS1** is on the energy summit along the potential energy surface (PES) as well. Therefore, this step can be regarded as the rate-determining step (RDS) along the stepwise pathway, which is compatible with the experimental results that the raction rate and the conversion of **2a** related to the amount of catalyst $ZnEt_2$ used.[14d] The high active Gibbs free energy of 98.6 kJ mol^{-1} indicates that $ZnEt_2$ shows poor catalytic performance on the allylation of **1a** with **2a**, which is in agreement with the experimental result that the reaction catalyzed by $ZnEt_2$ alone proceeded with lower conversion.[14d] Moreover, the calculations suggest that the formation of the four-coordinated boron center intermediate favors the activation of the B–C_α bond and the boron to zinc transmetalation. Hence, how to overcome the energetic bottleneck for the formation of the four-coordinated boron intermediate becomes very crucial for accelerating the reaction rate.

Role of EtOH in the reaction: Since the allylation of **1a** with **2a** catalyzed by a combination of $ZnEt_2$ and the additive EtOH was found to be more effective in the experiment, the catalytic mechanism of this process was studied to clarify the role of EtOH for accelerating the reaction rate.

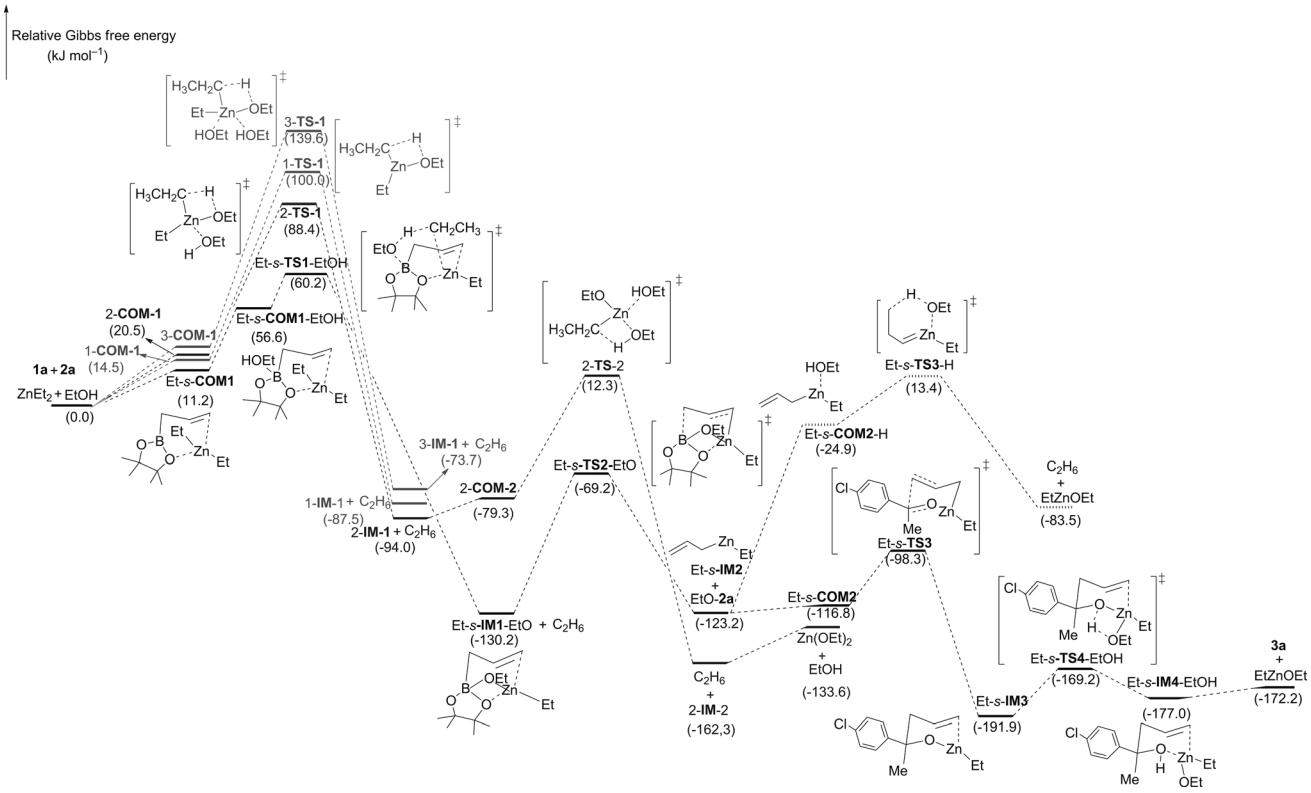

Figure 3. Energy profile of allylation of **1a** with **2a** catalyzed by $ZnEt_2$ and EtOH. The relative Gibbs free energies in THF at the M05-2X/6-311++G(d,p) level are given in kJ mol^{-1}.

The schematic structures along the reaction pathway catalyzed by $ZnEt_2$ and additive EtOH are illustrated in Figure S2 and S3 in the Supporting Information. The energy profile of the reaction pathway is shown in Figure 3.

According to related literature,[14] zinc oxidates are suggested to be competent to promote the boron to zinc transmetalation. Therefore, our calculations assume that the active species zinc alkoxide might be formed when the additive EtOH was added to the reaction system. Two possible mechanisms for the formation of zinc alkoxide species were located, respetively. As shown in Figure S2 and S3 in the Supporting Information, one corresponds to the direct generation of $Zn(OEt)_2$ from $ZnEt_2$ with excess EtOH, and the other corresponds to the formation of zinc alkoxide species mediated by the boron center of **2a**.

As shown in Figure 3, the direct formation of $Zn(OEt)_2$ from $ZnEt_2$ with excess EtOH undergoes stepwise proton transfer from EtOH to the ethyl group of $ZnEt_2$ with the release of two molecules ethane. For the first proton transfer step, three possible transition states 1-**TS**-1, 2-**TS**-1, and 3-**TS**-1 were located, respectively. Among these three transition states, the relative Gibbs free energy of 2-**TS**-1 is the lowest, indicating that the four-coordinated zinc transition state bearing the square pyramid structure is energetically more favorable than the three and five-coordinated zinc transition states. Hence, the second proton transfer may most probably take place via the four-coordinated zinc transition state 2-**TS**-2. The energy barriers for the two steps are calculated to be 67.9 and 91.6 kJ mol^{-1} in Gibbs free energies, respectively, which suggests that the formation of ethyl ethoxide zinc species is relatively facile to the generation of $Zn(OEt)_2$.

On the other hand, the zinc alkoxide species can be formed via the boron center of **2a** mediated pathway, which starts from the coordination of EtOH to the boron center of Et-*s*-**COM1** with the formation of the ternary complex Et-*s*-**COM1**-EtOH. In Et-*s*-**COM1**-EtOH, the O–H bond is weakened, verified by the longer O–H bond distance (1.027 Å vs. 0.961 Å in free EtOH) and the larger occupancy of antibonding orbital of BD*(σ) O–H (0.139 vs. 0.007 in free EtOH). From the high reactivity complex Et-*s*-**COM1**-EtOH, the proton transfer from the oxygen atom of EtOH to ethyl group of $ZnEt_2$ easily happens via the six-membered ring transition state Et-*s*-**TS1**-EtOH with much lower energy barrier of 3.6 kJ mol^{-1} in Gibbs free energy. In Et-*s*-**TS1**-EtOH, the large stabilization energy [BD*(σ)B–O → BD*(σ) O–H (85.3 kJ mol^{-1})] indicates that the dominate promotion occurs from boron moiety to O–H bond. As a result, the relative Gibbs free energy of Et-*s*-**TS1**-EtOH is 24.2 kJ mol^{-1} lower than that of 2-**TS**-1, which suggests that the proton transfer from the oxygen atom of EtOH to ethyl group of $ZnEt_2$ mediated by the boron center of **2a** is energetically favorable. Downhill from Et-*s*-**TS1**-EtOH, Et-*s*-**IM1**-EtO intermediate is yielded with the release of one

molecule ethane with an exothermicity of 130.2 kJ mol^{-1} in Gibbs free energy. In Et-*s*-**IM1**-EtO, the ethoxide group spontaneously coordinates to zinc atom with the Zn–O distance of 2.006 Å, meaning that the zinc alkoxide species is formed. This result is consistent with the ^{1}H NMR study that showed how $ZnEt_2$ was quickly converted to zinc alkoxide species when EtOH was added to the reaction system composed of $ZnEt_2$ and **2a**.[14d] For Et-*s*-**IM1**-EtO, the ethoxide group is bonded to the boron center, resulting in a four-coordinated boron center intermediate, which has been reported in theoretical calculations on the Suzuki–Miyaura reaction.[24] The interaction between the ethoxide group and the boron center favors the activation of B–C_α bond, suggested by the smaller Wiberg bond index (0.751) and the increased occupancy of antibonding orbital of BD*(σ) B–C_α (0.550). From Et-*s*-**IM1**-EtO, the boron to zinc transmetalation occurs via the six-membered ring transition state Et-*s*-**TS2**-EtO, leading to the formation of allylzincate active species Et-*s*-**IM2** and the release of one ethoxide boronate. The energy barrier for the boron to zinc transmetalation step is calculated to be 61.0 kJ mol^{-1} in Gibbs free energy. Since EtOH was added in the reaction system, the resulting allylzincate active species Et-*s*-**IM2** might alternatively react with ketone **1a** to afford allylation intermediate Et-*s*-**IM3** or undergo the protonolysis process by EtOH. The energy barrier for the addition of **1a** to Et-*s*-**IM2** via Et-*s*-**TS3** is 24.9 kJ mol^{-1}, which is much lower than that of the protonolysis process via transition state Et-*s*-**TS3**-H (136.6 kJ mol^{-1}). Thus, the allylation of ketone **1a** completely competes with protonolysis of allylzincate active species Et-*s*-**IM2** in thermodynamics and kinetics, and the allylation product would be achieved in high yield. Finally, EtOH can donate one proton to complete the protonation of Et-*s*-**IM3** via the transition state Et-*s*-**TS4**-EtOH with the lower energy barrier of 22.7 kJ mol^{-1} in Gibbs free energies. This protonation process is predicted to be more feasible than the boron to zinc transmetalation via the transition state Et-*s*-**TS4** ($\Delta G =$ 58.7 kJ mol^{-1}). The desired product homoallylic alcohol **3a** would be obtained by the direct dissociation of the Zn–O bond in the product complex Et-*s*-**IM4**-EtOH with recovery of catalytically active species ethyl ethoxide zinc (EtZnOEt).

Overall, from the energy profile in Figure 3, it is apparent that Et-*s*-**TS1**-EtOH with the relative Gibbs free energy of 60.2 kJ mol^{-1} is on the energy ummit along the PES. Once passing the transition state Et-*s*-**TS1**-EtOH, the active intermediate Et-*s*-**IM1**-EtO is generated and acted as the catalytically active species for the catalytic cycle. For the catalytic cycle, the step of boron to zinc transmetalation from Et-*s*-**IM1**-EtO to Et-*s*-**IM2** via the transtion state Et-*s*-**TS2**-EtO with the largest reaction barrier of 61.0 kJ mol^{-1} is regarded as the RDS. The reaction rate and the conversion of **2a** under such catalytic system should be controlled by the formation of Et-*s*-**IM1**-EtO via Et-*s*-**TS1**-EtOH as well as the boron to zinc transmetalation step from Et-*s*-**IM1**-EtO to Et-*s*-**IM2**. As compared to the reaction catalyzed by $ZnEt_2$ alone, the addition of EtOH is significantly in favor of lowering the energy barrier for the formation of the four-coordinated boron intermediate from 98.6 kJ mol^{-1} to 60.2 kJ mol^{-1} in Gibbs free energy. The computed results reasonably account for the experimental observation that the reaction rate is greatly accelerated when EtOH was added to the reaction system composed of $ZnEt_2$ and **2a**.[14d] Therefore, it can be concluded that the additive EtOH plays essential roles in: 1) the transformation of low catalytic activity $ZnEt_2$ into zinc alkoxide species with high catalytic activity for the boron to zinc transmetalation, 2) providing protons for the protonation of the product intermediate and accelerating the regeneration of the zinc alkoxide active species.

Factors influencing the reaction rate: Furthermore, to prove the reasonableness of the mechanism proposed for the above catalytic system and gain insight into more influencing factors for the present reaction, the allylation reaction between **1a** and a series of allylboronate reagents (**2a**–**2d** in Scheme 2) catalyzed by $ZnEt_2$ with different alcohol additives was investigated. The catalytic effect of several zinc compounds including $Zn(OEt)_2$, $Zn(OH)_2$, ZnF_2, $ZnCl_2$, and $ZnBr_2$ was also studied comparatively in this section.

Effect of alcohol additives: To study the effect of alcohol additives on the reaction, MeOH, *i*PrOH, and *t*BuOH were used as additives in our theoretical simulation. The reaction mechanisms for the allylation of **1a** with **2a** catalyzed by $ZnEt_2$ with the three additives were calculated at the same level and the energy profiles are summarized in Figure 4. As shown in Figure 4, the PESs of the reaction catalyzed by $ZnEt_2$ with the three additives are similar to the corresponding one in the case of EtOH as the additive. The first transition states (**TS1s**) are on the energy top along the PESs, and the steps of the boron to zinc transmetalation are RDSs for the catalytic cycles. The relative Gibbs free energy of **TS1s** are calculated to be 57.4, 60.2, 68.9, and 76.9 kJ mol^{-1}, and the energy barriers for the steps of the boron to zinc transmetalation are 55.3, 61.0, 64.1, and 59.4 kJ mol^{-1}, respectively. These calculations suggest that the alcohol additives might primarily affect the formation of zinc alkoxide species. Since the relative Gibbs free energy of Et-*s*-**TS1**-*t*BuOH is the highest among the four transition states, the allylation reaction between **1a** and **2a** catalyzed by $ZnEt_2$ with the additive *t*BuOH may proceed more slowly than with the other three additives. This result is in agreement with the experimental observations obtained when *t*BuOH was used as additive[14d] and further confirms the mechanism proposed above. For the four alcohols, NBO analysis shows that the charges on the proton of the hydroxyl group are 0.456 *e*, 0.453 *e*, 0.460 *e*, and 0.456 *e*, and the populations of antibonding orbital of BD*(σ) O–H are 0.006, 0.007, 0.006, 0.007, respectively. These comparable results indicate that the activities of the proton of hydroxyl group in the four alcohols are comparable with one another. Therefore, it can be predicted that the energy difference between the four transition states (**TS1s**) might be caused by the steric effect

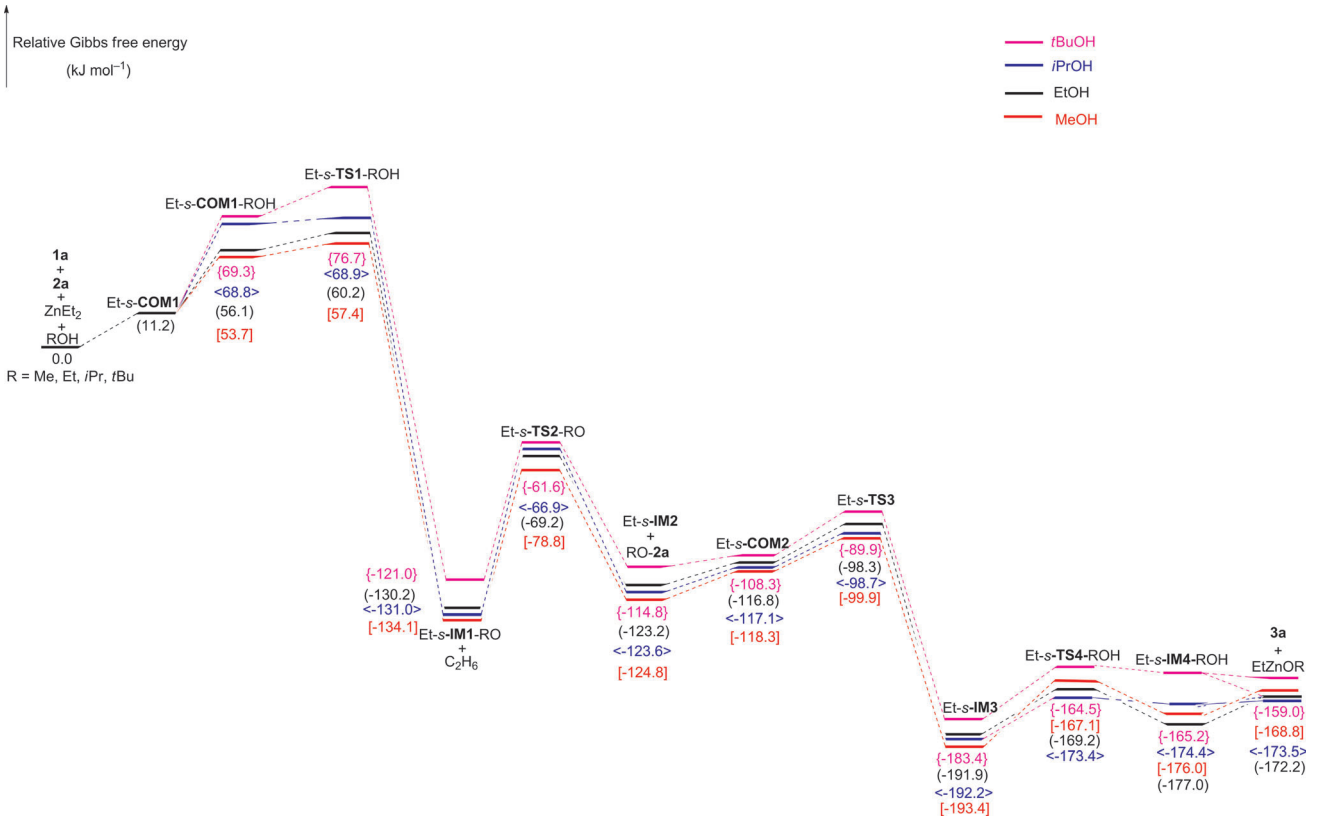

Figure 4. Energy profile of the allylation of **1a** with **2a** catalyzed by $ZnEt_2$ with the four alcohols. The relative Gibbs free energies in THF at the M05-2X/6-311++G(d,p) level are given in kJ mol^{-1}.

from the R groups of the alcohols. The alcohol with a less sterically encumbering R group should be the suitable additive for the present reaction.

Effect of allylboronate reagents: To investigate the effect of the allylboronates on the reaction, the methyl-substituted boronates **2b**, **2c**, and **2d** were employed as the allylboronate reagents for the allylation of **1a** catalyzed by $ZnEt_2$ and EtOH. For the methyl-substituted boronates **2d**, both *E* and *Z* configurations of **2d** were considered. The predicted mechanisms and energy profiles are presented in Figure 5. As shown in Figure 5, for the five allylboronates, the computed ΔG_1 for the formation of zinc alkoxide species are 60.2, 62.4, 50.7, 59.8, and 57.6 kJ mol^{-1}, and ΔG_2 for the boron to zinc transmetalation are 61.0, 57.9, 54.4, 79.9 and 72.1 kJ mol^{-1}, respectively. These computed results indicate that the methyl substituents on the allylboronates might play a main role in the step of the boron to zinc transmetalation. As compared to the boronate **2a**, the α-methyl-substituted boronate **2b** and β-methyl-substituted boronate **2c** are effective for the boron to zinc transmetalation, while the reactivity of the γ-methyl-substituted boronates (*E*/*Z*-**2d**) is relatively lower. These calculations are consistent with the experimental results obtained on the effect of substituents on allylboronates.[14d] NBO analysis for the five intermediates (**IM1s**) shows that the methyl groups substituted at C_γ position decrease the charges of the C_γ atom in *E*-**2d**-Et-*s*-**IM1**-EtO (0.332 *e*) and *Z*-**2d**-Et-*s*-**IM1**-EtO (0.330 *e*), which disfavors the insertion of the zinc to the C_γ=C_β bond. The structural analysis of the five transition states (**TS2s**) suggests that the transition states *E*-**2d**-Et-*s*-**TS2**-EtO and *Z*-**2d**-Et-*s*-**TS2**-EtO suffer more steric hindrance from the methyl groups substituted at C_γ position for the insertion of the zinc to the C_γ=C_β bond. For *E*-**2d**-Et-*s*-**TS2**-EtO, the methyl group located at the equatorial position suffers the larger repulsion from the ethyl group on the zinc center, which makes *E*-**2d**-Et-*s*-**TS2**-EtO more unstable than *Z*-**2d**-Et-*s*-**TS2**-EtO by 6.4 kJ mol^{-1} in Gibbs free energy. Therefore, it can be predicted that the terminally substituted allylboronate agents bear low reactivity for the boron to zinc transmetalation.

Catalytic effect of zinc compounds: Apart from the effects of additives and allylboronate reagents, different zinc compounds perform different catalytic effect for the allylation reaction as well. In Fandrick's experiment, $ZnCl_2$ and $ZnBr_2$ were used as the catalysts for the allylation of **1a** with **2a**, although the catalytic effect of $ZnCl_2$ and $ZnBr_2$ are inferior to the catalytic system composed of $ZnEt_2$ and EtOH.[14d] On the other hand, ZnF_2 and $Zn(OH)_2$ were proved to be competent for the allylation of imines and aldehydes with pinacol allylboronates by Kobayashi and co-workers.[14a–c] To clarify the catalytic mechanism and compare the catalytic capability of several zinc compounds for the allylation reac-

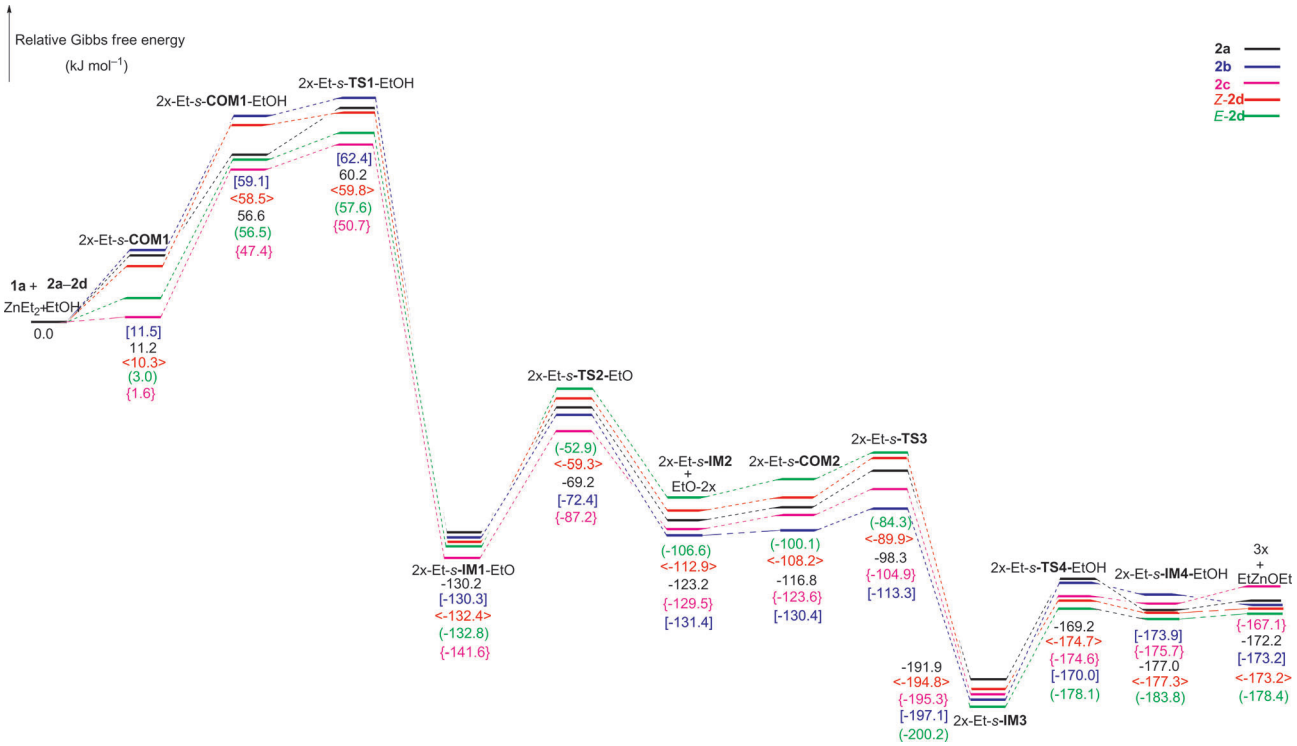

Figure 5. Energy profile of the allylation of **1a** with **2a**–**2d** catalyzed by $ZnEt_2$ with EtOH. The relative Gibbs free energies in THF at the M05-2X/6-311++G(d,p) level are given in kJ mol^{-1}.

tion, five zinc compounds including $Zn(OEt)_2$, $Zn(OH)_2$, ZnF_2, $ZnCl_2$, and $ZnBr_2$ were chosen as the catalysts for the allylation of **1a** with **2a** in our theoretical simulations. For the five zinc compounds-catalyzed allylation reactions, both double γ-addition stepwise mechanism and Lewis acid-catalyzed concerted mechanism were calculated and marked as *c*-path and *s*-path, respectively. To make a concise expression, the detailed reaction mechanism catalyze by $Zn(OEt)_2$ is shown in Figure 6 (other similar results are presented in the Supporting Information). The energy profile for the five reactions is summarized in Figure 7.

From the energy profile in Figure 7, it is clear that the reaction prefers to proceed with the double γ-addition stepwise mechanism when $Zn(OEt)_2$, $Zn(OH)_2$, and ZnF_2 are

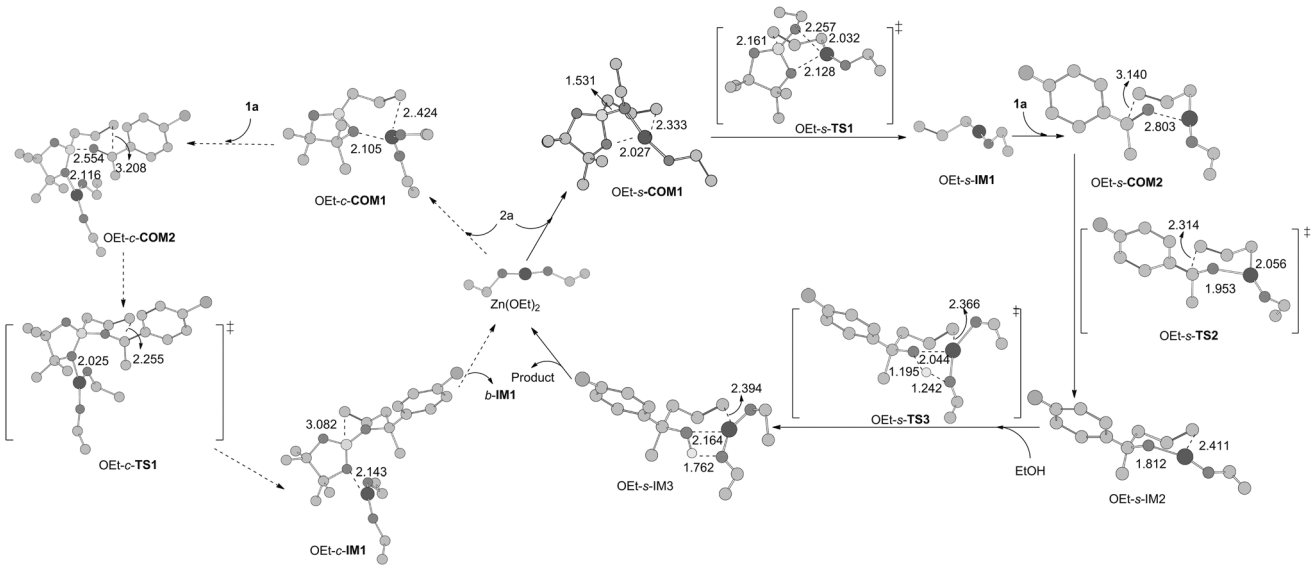

Figure 6. Schematic structures of the species in the allylation of **1a** with **2a** catalyzed by $Zn(OEt)_2$. Some H atoms are omitted for clarity. Bond lengths are given in Å.

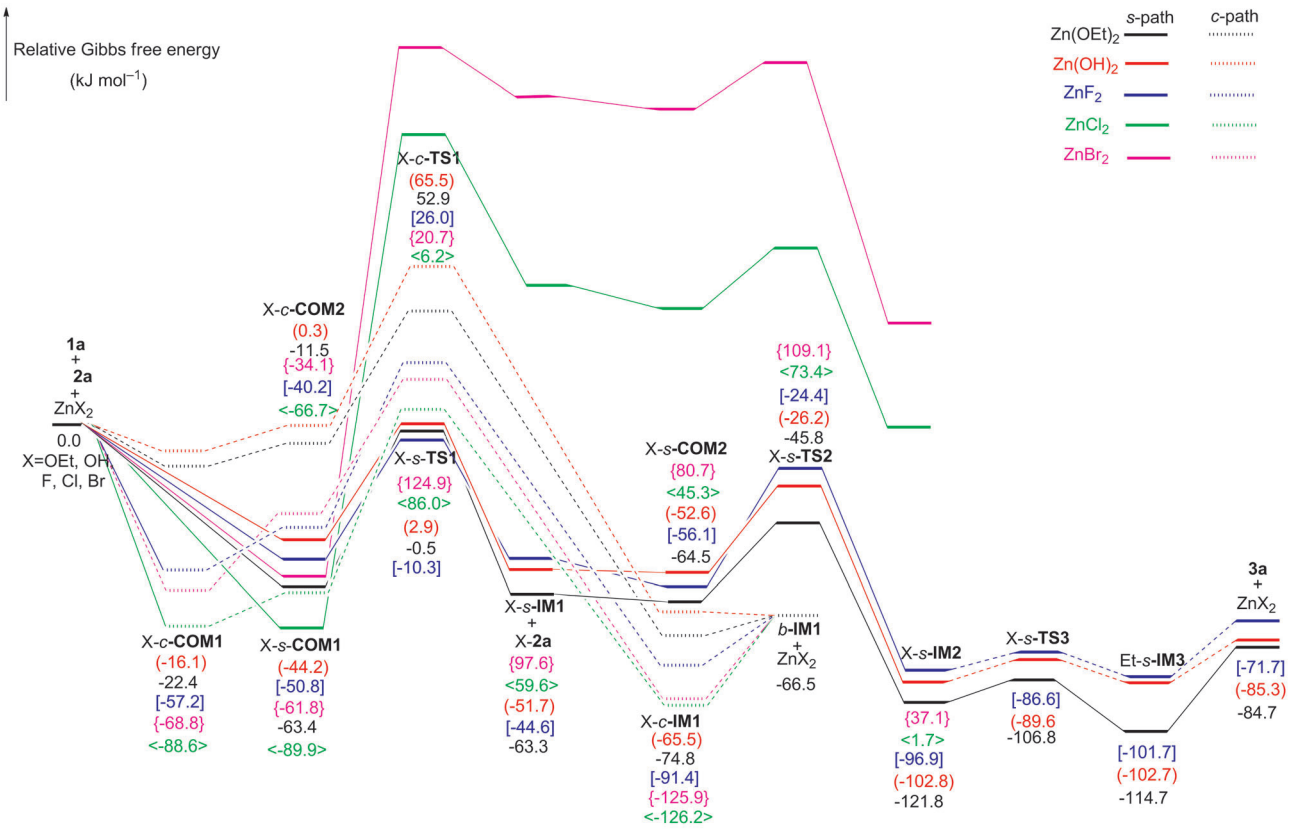

Figure 7. Energy profile of the allylation of **1a** with **2a** catalyzed by $Zn(OEt)_2$, $Zn(OH)_2$, ZnF_2, $ZnCl_2$, and $ZnBr_2$. The relative Gibbs free energies in THF at the M05-2X/6-311++G(d,p) level are given in kJ mol^{-1}.

used as catalysts. The RDS for the catalytic cycle is the boron to zinc transmetalation step, which is in line with the above theoretical results and kinetic studies by Kobayashi and co-workers.[14c] The energy barrier of the boron to zinc transmetalation catalyzed by $Zn(OEt)_2$ is comparable to the corresponding one catalyzed by $ZnEt_2$ with additive EtOH (62.9 kJ mol^{-1} vs. 61.0 kJ mol^{-1}), meaning that the catalytic effect of $Zn(OEt)_2$ and ethyl ethoxide zinc are equivalent. On the other hand, when the reaction is catalyzed by $ZnCl_2$ or $ZnBr_2$, the concerted mechanism is more favorable than the stepwise mechanism. To elucidate the reason for the different catalytic mechanisms, NBO analysis for the key complexes *s*-**COM1** was carried out.

As shown in Figure 8, the orbital interactions between the EtO, OH, and F groups of zinc compounds and the boron

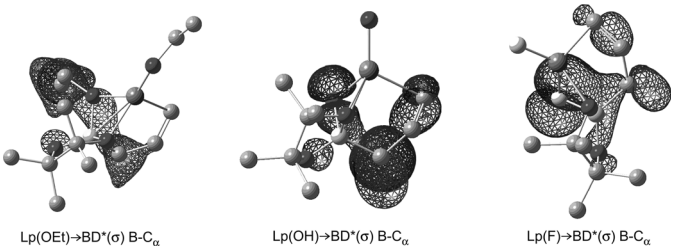

Figure 8. Visualization of the orbital interactions in complexes OEt-*s*-**COM1**, OH-*s*-**COM1**, and F-*s*-**COM1**.

atoms of **2a** are found in complexes OEt-*s*-**COM1**, OH-*s*-**COM1**, and F-*s*-**COM1**. These orbital interactions activates the B–C_α bond, which are verified by the decreased Wiberg bond index of the B–C_α bond and the increased population of antibonding orbital of BD*(σ) B–C_α bond in Table 1. As a result, the boron to zinc transmetalation including the cleavage of the B–C_α bond and the insertion of zinc to the C_γ=C_β bond can easily take place via the transition states OEt-*s*-**TS1**, OH-*s*-**TS1**, and F-*s*-**TS1**. On the contrary, for complexes Cl-*s*-**COM1** and Br-*s*-**COM1**, the orbital interactions between the chlorine or bromine atoms and boron atoms are not observed, which might be due to the fact that the lone pair electron on d orbital of chlorine or bromine atoms could not spontaneously match with the empty p orbital of boron atoms. Besides, the values of the negative charges on the C_γ atom and the positive charges on the zinc atom in Cl-*s*-**COM1** and Br-*s*-**COM1** are smaller than those in OEt-*s*-**COM1**, OH-*s*-**COM1**, and F-*s*-**COM1**, which also disfavors the insertion of zinc to the C_γ=C_β bond. For the lack of the activation of B–C_α bond in Cl-*s*-**COM1** and Br-*s*-**COM1**, the boron to zinc transmetalation accompanied by the transfer of chlorine and bromine to boron center at transition states Cl-*s*-**TS1** and Br-*s*-**TS1** requires much higher energy barriers of 175.9 and 186.7 kJ mol^{-1} in Gibbs free energies. Therefore, when $ZnCl_2$ or $ZnBr_2$ was used as the catalyst, the boron to zinc transmetalation did hardly occur.

Table 1. NBO analysis for complexes *s*-**COM1** at the M05-2X/6-311++G(d,p) level of theory.

Species	Charge [*e*]				B–C_α bond	
	B	C_α	C_γ	Zn	Wiber bond index	population of antibonding
2a	1.190	−0.803	−0.413	–	0.878	0.019
EtO-*s*-**COM1**	1.219	−0.798	−0.578	1.427	0.749	0.040
OH-*s*-**COM1**	1.152	−0.782	−0.579	1.387	0.764	0.053
F-*s*-**COM1**	1.186	−0.792	−0.592	1.450	0.773	0.050
Cl-*s*-**COM1**	1.231	−0.816	−0.485	1.048	0.871	0.021
Br-*s*-**COM1**	1.235	−0.825	−0.431	0.911	0.873	0.020

$ZnCl_2$ and $ZnBr_2$ tend to act as Lewis acids in the activation of the oxygen atom of boronates, which is similar to the activation mode proposed in the theoretical calculation of $AlCl_3$-catalyzed allylation of benzaldehyde.[7] The generation of the allylation product intermediate via the concerted transition states Cl-*c*-**TS1** and Br-*c*-**TS1** might be relatively feasible with the energy barriers of 94.8 and 89.5 kJ mol^{-1} in Gibbs free energies.

Finally, the catalytic capabilities of $Zn(OEt)_2$, $Zn(OH)_2$, ZnF_2, $ZnCl_2$, and $ZnBr_2$ for the allylation of **1a** with **2a** were evaluated by the turnover frequency (TOF) of the catalytic cycle based on the energetic span model (δE).[25] The energetic span model proposed by Kozuch and Shaik allows the estimation of the TOF of a catalytic reaction from its calculated energy profile. According to Equations (1) and (2)[26] and the energy profiles in Figure 7, the δE of the five reactions catalyzed by $Zn(OEt)_2$, $Zn(OH)_2$, ZnF_2, $ZnCl_2$, and $ZnBr_2$ are calculated to be 62.9, 41.7, 40.5, 94.8, and 89.5 kJ mol^{-1}, corresponding to the theoretical TOF values of 2.1×10^5, 1.1×10^9, 1.8×10^9, 5.5×10^{-1}, and 4.7 h^{-1}, respectively.

$$\mathrm{TOF} = \frac{\mathrm{E}k_\mathrm{b}T}{h}e^{-\frac{\delta E}{RT}} \quad (1)$$

$$\delta E = G_{\mathrm{TDTS}} - G_{\mathrm{TDI}} \text{ if TDTS appears after TDI} \quad (2a)$$

$$\delta E = \mathrm{G}_{\mathrm{TDTS}} - \mathrm{G}_{\mathrm{TDI}} + \Delta G_\mathrm{r} \text{ if TDTS appears before TDI} \quad (2b)$$

The TOFs of $Zn(OEt)_2$, $Zn(OH)_2$, and ZnF_2-catalytzed reactions are much larger than the corresponding ones in $ZnCl_2$ and $ZnBr_2$-catalyzed reactions, implying that $Zn(OEt)_2$, $Zn(OH)_2$, and ZnF_2 exhibit higher catalytic efficiency than $ZnCl_2$ and $ZnBr_2$ for the allylation reaction between carbonyl compounds and allylboronates. The theoretical calculations are in accordance with the experimental results.[14] It also predicts that zinc fluorides and zinc hydroxides with larger TOF values should be the better catalysts for the allylation of carbonyl compounds with allylboronates.

Conclusion

The mechanisms for the allylation of 4-chloroacetophenone and pinacol allylboronates catalyzed by $ZnEt_2$ with or without the additive alcohols have been theoretically investigated using DFT calculations at the M05-2X/6-311++G(d,p) level of theory. The major conclusions are listed as follows.

The calculations reveal that the reaction catalyzed by $ZnEt_2$ with the additive EtOH proceeds through a double γ-addition stepwise mechanism. The active intermediate with a four-coordinated boron center is initially formed through proton transfer from EtOH to the ethyl group of $ZnEt_2$ mediated by the boron center of pinacol allylboronates. The catalytic cycle involves the boron to zinc transmetalation, the addition of ketone to the allylzincate species, and the formation of the final product with the recovery of catalytic active species ethyl ethoxide zinc. The boron to zinc transmetalation with the largest energy barrier of 61.0 kJ mol^{-1} is predicted to be the RDS for the catalytic cycle. As compared with the reaction catalyzed by $ZnEt_2$ alone, the additive EtOH plays key roles in: 1) lowering the activation Gibbs free energy (from 98.6 kJ mol^{-1} to 60.2 kJ mol^{-1}) for the formation of the four-coordinated boron active intermediate, 2) transforming the low catalytic activity $ZnEt_2$ into high activity zinc alkoxide species.

The calculations indicate that the additive alcohols might primarily affect the formation of the four-coordinated active intermediate, and the alcohol with a less sterically encumbering R group might be the suitable additive for the present reaction. The substituent groups on the allylboronates play an important role in the step of boron to zinc transmetalation, and the allylboronates with the substituents on the C_γ atom are less reactive for the allylation reaction.

The comparison of the catalytic effect between the zinc compounds studied suggests that $Zn(OEt)_2$, $Zn(OH)_2$, and ZnF_2 are in favor of the boron to zinc transmetalation, which might be due to the activation of the B–C_α bond through the interactions between the p orbitals of OEt, OH, and F groups of the zinc compounds and the empty p orbital of the boron center of **2a**. The zinc fluorides and zinc hydroxides are predicted to be the more efficient catalysts for the allylation of carbonyl compounds with allylboronates.

Acknowledgements

We thank the National Natural Science Foundation of China (Nos. 21102096 and 21021001).

[1] For recent reviews, see: a) S. E. Denmark, J. Fu, *Chem. Rev.* **2003**, *103*, 2763–2794; b) M. Hatano, K. Ishihara, *Synthesis* **2008**, 1647–1675; c) M. Yus, J. C. González-Gómez, F. Foubelo, *Chem. Rev.* **2011**, *111*, 7774–7854.

[2] For selected examples of allylhalides as allylating reagent, see: a) K. T. Tan, S. S. Chng, T. P. Loh, *J. Am. Chem. Soc.* **2003**, *125*, 2958–2963; b) J. H. Dam, P. Fristrup, R. Madsen, *J. Org. Chem.* **2008**, *73*, 3228–3235; c) L. M. Zhao, H. S. Jin, L. J. Wan, L. M.

Zhang, *J. Org. Chem.* **2011**, *76*, 1831–1837; d) L. M. Zhao, L. J. Wan, H.-S. Jin, S.-Q. Zhang, *Eur. J. Org. Chem.* **2012**, 2579–2584.

[3] For selected examples of allylsilanes as allylating reagent, see: a) M. Wadamoto, N. Ozasa, A. Yanagisawa, H. Yamamoto, *J. Org. Chem.* **2003**, *68*, 5593–5601; b) M. Wadamoto, H. Yamamoto, *J. Am. Chem. Soc.* **2005**, *127*, 14556–14556; c) K. Takeuchi, T. Takeda, T. Fujimoto, I. Yamamoto, *Tetrahedron* **2007**, *63*, 5319–5322; d) A. Kadlčíková, I. Valterová, L. Ducháčková, J. Roithová, M. Kotora, *Chem. Eur. J.* **2010**, *16*, 9442–9445; e) A. V. Malkov, O. Kysilka, M. Edgar, A. Kadlčíková, M. Kotora, P. Kočovský, *Chem. Eur. J.* **2011**, *17*, 7162–7166; f) G. Rouquet, F. Robert, R. Méreau, F. Castet, Y. Landais, *Chem. Eur. J.* **2011**, *17*, 13904–13911; g) W. A. Chalifoux, S. K. Reznik, J. L. Leighton, *Nature* **2012**, *487*, 86–89.

[4] For selected examples of allylstannanes as allylating reagent, see: a) H. Hanawa, T. Hashimoto, K. Maruoka, *J. Am. Chem. Soc.* **2003**, *125*, 1708–1709; b) J. G. Kim, K. M. Waltz, I. F. Garcia, D. Kwiatkowski, P. J. Walsh, *J. Am. Chem. Soc.* **2004**, *126*, 12580–12585; c) A. J. Wooten, J. G. Kim, P. J. Walsh, *Org. Lett.* **2007**, *9*, 381–384; d) M. Kojima, K. Mikami, *Chem. Eur. J.* **2011**, *17*, 13950–13953; e) Z. Li, B. Plancq, T. Ollevier, *Chem. Eur. J.* **2012**, *18*, 3144–3147.

[5] For selected examples of allylboronates as allylating reagent, see: a) H. Yamamoto, K. Futatsugi, *Angew. Chem.* **2005**, *117*, 1958–1977; *Angew. Chem. Int. Ed.* **2005**, *44*, 1924–1942; b) D. S. Barnett, P. N. Moquist, S. E. Schaus, *Angew. Chem.* **2009**, *121*, 8835–8838; *Angew. Chem. Int. Ed.* **2009**, *48*, 8679–8682; c) J. W. J. Kennedy, D. G. Hall, *Angew. Chem.* **2003**, *115*, 4880–4887; *Angew. Chem. Int. Ed.* **2003**, *42*, 4732–4739; d) Y. Yamamoto, S. Yamada, H. Nishiyama, *Chem. Eur. J.* **2012**, *18*, 3153–3156; e) M. Gravel, H. Lachace, X. S. Lu, D. G. Hall, *Synthesis* **2004**, 1290–1302; f) H. Lachance, M. St-Onge, D. G. Hall, *J. Org. Chem.* **2005**, *70*, 4180–4183; g) L. Carosi, H. Lachance, D. G. Hall, *Tetrahedron Lett.* **2005**, *46*, 8981–8985.

[6] a) J. W. J. Kennedy, D. G. Hall, *J. Am. Chem. Soc.* **2002**, *124*, 11586–11587; b) H. Lachance, X. Lu, M. Gravel, D. G. Hall, *J. Am. Chem. Soc.* **2003**, *125*, 10160–10161; c) V. Rauniyar, D. G. Hall, *J. Am. Chem. Soc.* **2004**, *126*, 4518–4519; d) J. W. J. Kennedy, D. G. Hall, *J. Org. Chem.* **2004**, *69*, 4412–4428; e) D. G. Hall, *Synlett* **2007**, 1644–1655; f) T. Ishiyama, T. Ahiko, N. Miyaura, *J. Am. Chem. Soc.* **2002**, *124*, 12414–12415.

[7] K. Sakata, H. Fujimoto, *J. Am. Chem. Soc.* **2008**, *130*, 12519–12526.

[8] a) S. H. Yu, M. J. Ferguson, R. McDonald, D. G. Hall, *J. Am. Chem. Soc.* **2005**, *127*, 12808–12809; b) V. Rauniyar, D. G. Hall, *Angew. Chem.* **2006**, *118*, 2486–2488; *Angew. Chem. Int. Ed.* **2006**, *45*, 2426–2428; c) V. Rauniyar, H. Zhai, D. G. Hall, *J. Am. Chem. Soc.* **2008**, *130*, 8481–8490.

[9] P. Jain, J. C. Antilla, *J. Am. Chem. Soc.* **2010**, *132*, 11884–11886.

[10] M. N. Grayson, S. C. Pellegrinet, J. M. Goodman, *J. Am. Chem. Soc.* **2012**, *134*, 2716–2722.

[11] a) P. V. Ramachandran, D. Pratihar, D. Biswas, *Chem. Commun.* **2005**, 1988–1989; b) U. Schneider, S. Kobayashi, *Angew. Chem.* **2007**, *119*, 6013–6016; *Angew. Chem. Int. Ed.* **2007**, *46*, 5909–5912; c) U. Schneider, M. Ueno, S. Kobayashi, *J. Am. Chem. Soc.* **2008**, *130*, 13824–13825.

[12] a) R. Wada, K. Oisaki, M. Kanai, M. Shibasaki, *J. Am. Chem. Soc.* **2004**, *126*, 8910–8911; b) S. L. Shi, L. W. Xu, K. Oisaki, M. Kanai, M. Shibasaki, *J. Am. Chem. Soc.* **2010**, *132*, 6638–6639.

[13] P. Zhang, J. P. Morken, *J. Am. Chem. Soc.* **2009**, *131*, 12550–12551.

[14] a) M. Fujita, T. Nagano, U. Schneider, T. Hamada, C. Ogawa, S. Kobayashi, *J. Am. Chem. Soc.* **2008**, *130*, 2914–2915; b) S. Kobayashi, T. Endo, U. Schneider, M. Ueno, *Chem. Commun.* **2010**, *46*, 1260; c) S. Kobayashi, T. Endo, M. Ueno, *Angew. Chem. Int. Ed.* **2012**, *51*, 7431; d) K. R. Fandrick, D. R. Fandrick, J. J. Gao, J. T. Reeves, Z. L. Tan, W. J. Li, J. H. J. Song, B. Lu, N. K. Yee, C. H. Senanayake, *Org. Lett.* **2010**, *12*, 3748–3751.

[15] a) Y. Zhao, D. G. Truhlar, *Acc. Chem. Res.* **2008**, *41*, 157–167; b) E. G. Hohenstein, S. T. Chill, C. D. Sherrill, *J. Chem. Theory Comput.* **2008**, *4*, 1996–2000; c) M. D. Wodrich, C. Corminboeuf, P. R. Schreiner, A. A. Fokin, P. von R. Schleyer, *Org. Lett.* **2007**, *9*, 1851–1854.

[16] a) E. A. Amin, D. G. Truhlar, *J. Chem. Theory Comput.* **2008**, *4*, 75–85; b) A. Sorkin, D. G. Truhlar, E. A. Amin, *J. Chem. Theory Comput.* **2009**, *5*, 1254–1265; c) L. Schiaffino, G. Ercolani, *Chem. Eur. J.* **2010**, *16*, 3147–3156; d) C. M. Mayhan, T. J. Szabo, J. E. Adams, C. A. C. Deakyne, *Comput. Theor. Chem.* **2012**, *984*, 19–35.

[17] a) R. Ditchfield, W. J. Hehre, J. A. Pople, *J. Chem. Phys.* **1971**, *54*, 724–728; b) W. J. Hehre, R. Ditchfield, J. A. Pople, *J. Chem. Phys.* **1972**, *56*, 2257–2261; c) P. C. Hariharan, J. A. Pople, *Mol. Phys.* **1974**, *27*, 209–214; d) M. S. Gordon, *Chem. Phys. Lett.* **1980**, *76*, 163–168; e) P. C. Hariharan, J. A. Pople, *Theor. Chim. Acc.* **1973**, *28*, 213–222; f) J. P. Blaudeau, M. P. McGrath, L. A. Curtiss, L. Radom, *J. Chem. Phys.* **1997**, *107*, 5016–5021; g) M. M. Francl, W. J. Pietro, W. J. Hehre, J. S. Binkley, M. S. Gordon, D. J. DeFrees, J. A. Pople, *J. Chem. Phys.* **1982**, *77*, 3654–3655; h) R. C. Binning, Jr., L. A. Curtiss, *J. Comput. Chem.* **1990**, *11*, 1206–1209; i) V. A. Rassolov, J. A. Pople, M. A. Ratner, T. L. Windus, *J. Chem. Phys.* **1998**, *109*, 1223–1229; j) V. A. Rassolov, M. A. Ratner, J. A. Pople, P. C. Redfern, L. A. Curtiss, *J. Comput. Chem.* **2001**, *22*, 976–984.

[18] a) A. E. Reed, F. Weinhold, *J. Chem. Phys.* **1985**, *83*, 1736–1740; b) A. E. R. Reed, B. Weinstock, F. Weinhold, *J. Chem. Phys.* **1985**, *83*, 735–746; c) A. E. Reed, L. A. Curtiss, F. Weinhold, *Chem. Rev.* **1988**, *88*, 899–926; d) A. E. Reed, P. R. Schleyer, *J. Am. Chem. Soc.* **1990**, *112*, 1434–1445.

[19] M. Cossi, G. Scalmani, N. Rega, V. Barone, *J. Chem. Phys.* **2002**, *117*, 43–54.

[20] M. J. Frisch, et al. *Gaussian 03*, reversion E.01; Gaussian Inc.: Pittsburgh, PA, **2003**.

[21] C. Jimeno, S. Sayalero, T. Fjermestad, G. Colet, F. Maseras, M. A. Pericàs, *Angew. Chem.* **2008**, *120*, 1114–1117; *Angew. Chem. Int. Ed.* **2008**, *47*, 1098–1101.

[22] a) L. R. Domingo, J. A. Sáez, *Org. Biomol. Chem.* **2009**, *7*, 3576–3583; b) L. R. Domingo, E. Chamorro, P. Pérez, *J. Org. Chem.* **2008**, *73*, 4615–4624; c) R. G. Parr, L. von Szentpály, S. Liu, *J. Am. Chem. Soc.* **1999**, *121*, 1922–1924; d) L. R. Domingo, M. José Aurell, P. Pérez, R. Contreras, *Tetrahedron* **2002**, *58*, 4417–4423; e) Y. Yamaguchi, Y. Osamura, H. F. Schaefer, *J. Am. Chem. Soc.* **1983**, *105*, 7506; f) R. G. Parr, W. Yang, *Density Functional Theory of Atoms and Molecules,* Oxford University Press, New York, **1989**.

[23] The global electrophilicity index ω,[22c,d] which measures the stabilization energy when the system acquires an additional electronic charge ΔN from the environment, is given in terms of the electronic chemical potential μ and chemical hardness η by the following simple expression:[22e] $\omega[\mathrm{eV}]=(\mu^2/2\eta)$. Both quantities can be calculated in terms of the HOMO and LUMO electron energies, ε_H and ε_L, as $\mu\approx(\varepsilon_H+\varepsilon_L)/2$ and $\eta\approx(\varepsilon_H+\varepsilon_L)$, respectively.[22f] The nucleophilicity index N,[22b] based on the HOMO energies obtained within the Kohn–Sham scheme, is defined as $N=E_{\mathrm{HOMO(Nu)}}-E_{\mathrm{HOMO(TCE)}}$.[22b] The nucleophilicity is taken relative to tetracyanoethylene (TCE) as a reference, because it has the lowest HOMO energy in a large series of molecules already investigated in the context of polar cycloadditions.

[24] A. A. Braga, C. N. Morgon, H. G. Ujaque, F. Maseras, *J. Am. Chem. Soc.* **2005**, *127*, 9298–9307.

[25] a) S. Kozuch, S. Shaik, *J. Am. Chem. Soc.* **2006**, *128*, 3355–3365; b) S. Kozuch, S. Shaik, *J. Phys. Chem. A* **2008**, *112*, 6032–6041; c) A. Uhe, S. Kozuch, S. Shaik, *J. Comput. Chem.* **2011**, *32*, 978–985; d) S. Kozuch, S. Shaik, *Acc. Chem. Res.* **2011**, *44*, 101–110.

[26] G_{TDTS} and G_{TDI} are the Gibbs energies of the TOF determining transition state (TDTS) and the TOF determining intermediate (TDI), and ΔG_r is the global free energy of the whole cycle.

Received: August 12, 2012
Published online: November 14, 2012

